Composite Structures 209 (2019) 694–699

Contents lists available at ScienceDirect

Composite Structures

journal homepage: www.elsevier.com/locate/compstruct

Lightning strike and delamination performance of metal tufted carbon composites

D.M. Lombetti, A.A. Skordos*

School of Aerospace, Transport and Manufacturing, Cranfield University, Cranfield MK43 0AL, UK

ARTICLE INFO

Keywords:
Hybrid composites
Delamination
Lightning strike
Electrical properties
Tufting

ABSTRACT

This paper reports the development of multifunctional composites based on the use of metallic tufting. Stainless steel and copper are used to modify the through thickness mechanical and electrical behaviour of epoxy/carbon composites. The mechanical performance is evaluated in mode I delamination and the electrical behaviour is assessed using conductivity measurements and lightning strike tests. Metal tufting improves the delamination resistance by approximately 200% and 100% and the through thickness conductivity by 250 and 20 times for copper and stainless steel reinforcement, respectively. Lightning strike damage is suppressed significantly, with internal damage decreasing by about 90% and 75% compared to unprotected laminates for copper and stainless steel tufting, respectively. In the case of copper tufting the protection is comparable to what is achieved by standard surface copper mesh. These findings show that copper tufted composites are an ideal solution in applications requiring advanced mechanical and electrical functionality.

1. Introduction

In contrast to their high in-plane performance, composite materials are likely to undergo cracking at ply interfaces under out-of-plane loading, leading to interlaminar delamination. The use of reinforcing elements inserted through the thickness of the composite, sometimes referred to as micro-fasteners, such as Z-pins, stitches or tufts increases the out-of-plane toughness and improves the delamination resistance of composites [1–6]. In general, through-the-thickness reinforcement (TTR) of polymer matrix composites by the process of robotic tufting suppresses delamination by arresting the crack propagation and increases the delamination toughness by up to 25 times in mode I [7] and 200% in mode II [8] and the compression after impact (CAI) strength by up to 45% [9] compared to unreinforced materials.

The efficiency and effectiveness of tufting is governed by the thread material. Aramid thread is the most robust [10] and easiest option in terms of manufacturing. However, its use is not always desirable especially in aerospace structures due to its susceptibility to environmental degradation. Significant improvements of delamination resistance have been achieved with carbon [5,6,11,12]; however, this type of thread suffers from robustness problems during processing [13]. Glass threads present a satisfactory combination of performance [1,7,14] and manufacturability. Metal threads have not been used for tufting of composite structures but the typical strength and ductility associated with metals offer the potential for significant improvement of the delamination behaviour of tufted composite materials.

In addition to its ability of reinforcing monolithic composite structures in the through-the-thickness direction, tufting can potentially be used for the reinforcement of composite joints as well as joints of dissimilar materials. Applications around the integration of stiffening elements with composite skins are feasible, whilst potential use of metal tufting threads can enhance the behaviour of composite/metal joints. Currently, structural subcomponents, integrated in structures with high load bearing capabilities are joined together by mechanical fasteners [15]. The use of fasteners has an adverse effect on mechanical performance of the joined subcomponents due to the openings introduced and the associated local damage and stress concentrations, as well as on weight and manufacturing complexity [16,17].

The utilisation of composites in aerospace structures, which is mainly driven by their mechanical characteristics and associated weight benefits, is associated with challenges related to the electrical behaviour of these materials. The low electrical conductivity of carbon composites in the through thickness direction compared to their metallic counterparts makes their response to lightning strike problematic. The solution adopted in the industry is to integrate metallic elements in composite structures in the form of meshes, foils or interwoven fabrics attached to the surface of the component. These protective elements dissipate the current through the surface of the component and

* Corresponding author.
E-mail address: a.a.skordos@cranfield.ac.uk (A.A. Skordos).

https://doi.org/10.1016/j.compstruct.2018.11.005
Received 5 February 2018; Received in revised form 28 October 2018; Accepted 2 November 2018
Available online 03 November 2018

minimise or eliminate direct and indirect lightning strike damage. Studies using non-woven aluminium or copper mesh [18,19], interwoven phosphorous-bronze mesh [18], nickel coated carbon fibres [20] and aluminium interwoven fabric [21], show reduced surface and internal damage with increasing conductivity of the metal. In the best case scenario damage is limited to degradation of the paint and metal protection using aluminium mesh, nickel coated carbon fibres and aluminium interwoven fabric [18,20,21]. This is followed by burn-through of the composite with increasing diameter of the internal and surface damage for copper and phosphorous-bronze mesh [18]. The integration of metallic elements comes at a cost linked to the addition of an extra manufacturing step for the integration of the mesh. Furthermore, potential repair of the structural component due to lightning strike or other types of damage becomes more challenging and costly as the removed protection layer needs to be replaced and the added material connected electrically to the rest of the protective layer.

This paper focuses on the utilisation of metallic tufting as a multifunctional solution improving both through thickness mechanical and electrical properties of composites. Copper and stainless steel are utilised to tuft carbon/epoxy composites. The through thickness mechanical performance of the new materials is evaluated in mode I delamination and the associated damage mechanisms are investigated using microscopy. The electrical conductivity of the metal tufted composites is measured and correlated with the response in Zone 2A lightning strike tests. The overall lightning strike performance of the new materials is compared with the performance of both copper mesh protected and unprotected composites.

2. Materials and methods

2.1. Materials and specimens manufacture

Double cantilever beam (DCB) specimens were produced using a pseudo-unidirectional carbon fabric (Hexcel® G1157 D1300) with an areal density of 277 g/m^2. The material comprises carbon fibre tows (TENAX E HTA40 E13 6K) and a small amount (3 wt%) of glass fibre binder tow (EC9 34 Z40 1383). The fabric also contains 2.5 wt% of powder binder. This material was selected for delamination testing as it provides an architecture as close as possible to fully unidirectional for fabrics processed through a liquid composite moulding route. Twenty-four layers of the fabric were used to produce plates of unidirectional material. A 61 mm wide 10 μm thick PTFE film was inserted in the mid-plane of the plates to act as a crack starter during delamination testing. The preforms were reinforced by tufting using a stainless steel thread (Tibtech Thermotech N-30, AISI 316L) and an annealed copper wire (Goodfellow Ltd.). The tuft characteristics are summarised in Table 1. The tufting was carried out using a KSL KL 150 tufting head mounted on a 6-axis Kawasaki FS 20N robot. The tuft pattern was square with an areal tuft density of 0.5% corresponding to a tuft pitch of 3.5 mm for the stainless steel thread and 4.3 mm for the copper wire. A stack of 10 central plies was tufted and then incorporated within 24 layers of the fabric ensuring symmetry around the mid plane. The first tuft row was inserted at a distance of 15 mm from the crack starter film (Fig. 1). The preforms were impregnated with HexFlow® RTM6 epoxy resin using resin transfer moulding (RTM) to ensure a consistent nominal thickness of 6 mm across all specimens. The moulding was carried out in a heated square cavity with dimensions of 200 × 200 × 6 mm using an Isojet RTM injection piston. A pressure of 2 bar was utilised during the injection and the temperature was kept at 80 °C in the piston and 120 °C in the mould. The plates were cured at 160 °C for 75 min upon completion of impregnation and then de-moulded and post-cured at 180 °C for 120 min freestanding in a fan oven. Three panels were produced: an unreinforced carbon laminate, a stainless steel reinforced carbon laminate and a copper reinforced laminate. The plates were cut to the appropriate specimen dimensions (170 × 20 × 6 mm) using a diamond impregnated saw blade and aluminium blocks (15.5 × 20 × 8 mm) were bonded on them using Huntsman Araldite® 420 A/B.

Table 1
Tufting material properties.

Material	Steel	Copper
Type	Thermotech N-30, AISI 316L	Annealed copper
Filament count	2 × 180	1
Linear weight (g/km)	240	438
Fibre density (g/cm^3)	7.9	8.9
Cross sectional area (mm^2)	0.03	0.05

Electrical and lightning strike tests were carried out on carbon composite panels made of 4 layers of non-crimp bi-axial [± 45]$_s$ fabric plies (OCV™ Technical Fabrics C-BX440), (Toray T700 12 k) with an areal weight of 440 g/m^2. This material offers an appropriate reference for lightning strike testing as it provides a good response under biaxial loading and a highly reproducible fibre architecture governing electrical current dissipation. The preforms were tufted through the whole thickness with a pitch of 3 mm to minimise local effects in these tests and infused using vacuum assisted resin transfer moulding (VARTM) with HexFlow® RTM6 epoxy resin at 120 °C on an ELKOM heated platen. The material was cured following the same cure cycle as in the case of delamination specimens. Four panels were produced: an unreinforced unprotected carbon laminate, an unreinforced copper mesh protected (square pattern, wire diameter: 80 μm, areal weight: 100 g/m^2), a stainless steel reinforced carbon laminate and a copper reinforced laminate. In the case of the protected panel the metallic mesh was inserted as a surface layer prior to the infusion of the composite plate. The cured panels were trimmed along the edges in order to obtain a final size of 320 × 320 × 4 mm. Electrical conductivity tests were carried out on small coupons (20 × 20 × 4 mm). The electrically insulating resin rich layers on top and bottom surfaces were removed using 2400 grit paper without damaging the tuft seams and loops and the copper mesh in order to establish good electrical contact with the electrodes in conductivity measurements.

2.2. Testing methods

DCB specimens were painted and marked every millimetre on one side in order to record the crack length. The mode I tests were carried out on the electro-mechanical Zwick Z010 test machine with a 2 kN load cell. The test procedure followed the British Standard BS ISO 15024:2001. Five specimens were tested for each case. During the tests the applied load and crosshead displacement were recorded automatically and the crack length was determined visually and recorded alongside the corresponding load and displacement regularly. The initiation fracture toughness was determined using the 5%/max point. The corrected beam theory (CBT) was used to analyse the data. Correction factors were taken into account to compensate for the rotation at the delamination front due to asymmetrical specimen clamping, stiffening and rotation due to loading blocks and reduction of the lever arm at large displacements due to rotation at the end of the specimen. The fracture surfaces were analysed using scanning electron microscopy (SEM, Philips, XL 30 SFEG) of sputtered 10 × 15 mm samples and optical microscopy (Nikon stereo microscope, Nikon Eclipse ME600) of entire half beams to determine the failure mechanism and tuft behaviour.

The through the thickness electrical conductivity was measured using a combination of a precision DC current source (Keithley 6220) and a nanovoltmeter (Keithley 2182A) operating in delta mode. The specimens were placed in a measurement cell comprising two copper cylinders at an adjustable distance. Electrical contact was facilitated by the insertion of 10 μm thick copper foil between the two specimen surfaces and the copper cylinder and the application of a light compression force to the whole assembly. In these tests, the current was initially set at the minimum value (1nA) and then increased gradually

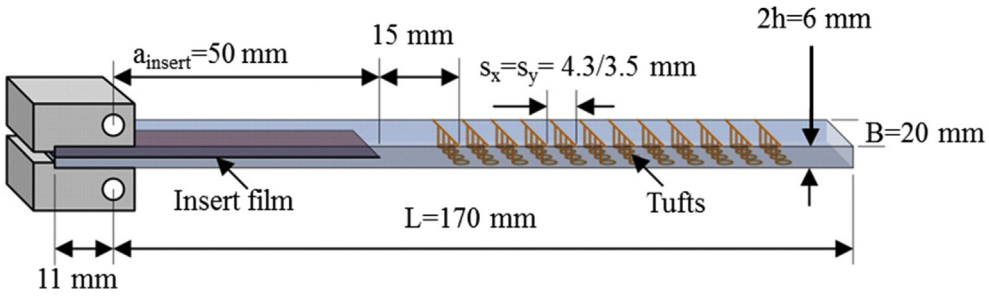

Fig. 1. Schematic of DCB specimens.

until the resistance measurement was stabilised. The stabilisation occurred at a current level that was typically 1–10 mA. This procedure was controlled using an in-house Labview code. The conductivity was calculated using the measured resistance and the geometry of the specimens. Measurements of the tufting materials conductivity were also carried out. This was performed by connecting two ends of a 2 m long segment of thread or wire to the setup and measuring the resistance.

The lightning strike tests were carried out at Cobham Antenna Systems, Lightning Testing Services, Abingdon, UK. The specimens were subjected to simulated Zone 2A lightning strikes following standard MIL-STD-1757A [36], comprising three current components: the slow waveforms B and C and the fast waveform D (Fig. 2). Component B has an average current amplitude of 2 kA with a maximum duration of 5 ms. This is followed by component C with a current amplitude of 200–800 A and a duration of 0.25–1 s. Component D is considered as the restrike with current reaching approximately 100 kA with a duration of maximum 500 µs. After the lightning strike tests the panels were analysed for internal and surface damage using ultrasound C-scanning (Structural Diagnostics Inc., Model 3510). Each panel was immersed in a water bath. The entire panel was scanned at 2–10 MHz with a resolution of 0.25 × 0.25 mm with the probe facing normally to the damaged surface.

3. Results and discussion

3.1. Delamination performance

The load-displacement curves of unreinforced, copper tufted and steel tufted material, illustrated in Fig. 3, show the same characteristics in the initial part: crack initiation occurs at a load between 90 N and 110 N. From that point on the crack propagates through the initial untufted region followed by a linear increase in load up to approximately 125 N in unreinforced and 110 N in tufted specimens. At 125 N the load of the control specimens starts decreasing continuously until specimen fracture, whilst in tufted specimens the crack is shortly arrested by the first tuft row (dotted line) followed by slow propagation to

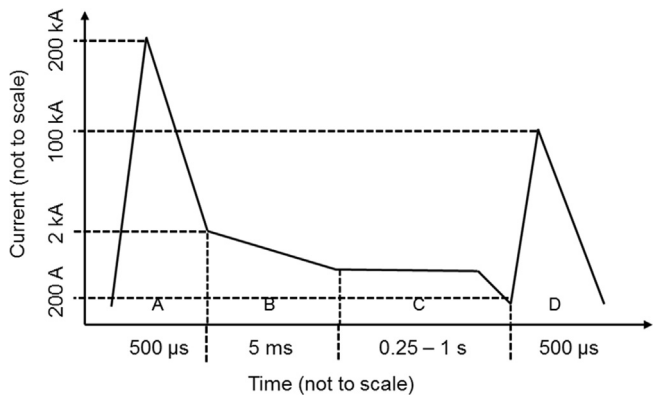

Fig. 2. Components of current waveform.

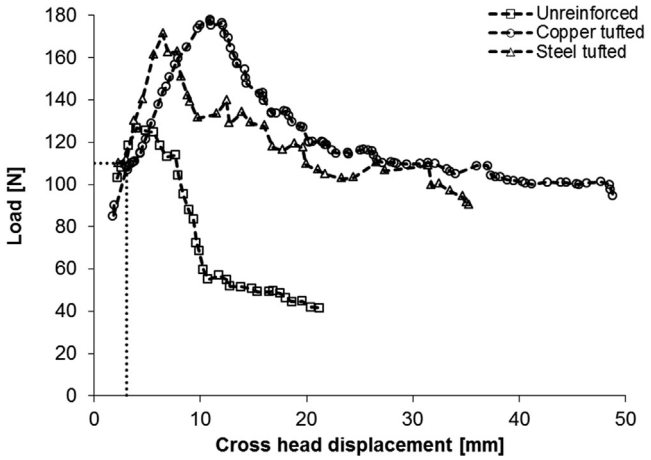

Fig. 3. Representative load-displacement curve of bindered composites tufted with copper and stainless steel.

the second or third tuft row in stainless steel tufted specimens, and fifth or sixth row in copper tufted specimens, leading to a linear increase in load up to the peaks of 171 N and 178 N for stainless steel and copper tufted specimens, respectively. Once the first tuft row ruptures, the high amount of energy accumulated is partially released so that the crack propagates abruptly, breaking up to two more tuft rows before being arrested by tufts leading to a decrease in load. This behaviour continues until final fracture of the specimen with relatively low variations in load during the entire delamination process, caused by periodic crack arrests and fibre bridging and undulation, both leading to an increase in load. It should be noted that during loading all specimens showed a symmetric response; no twisting occurred, whilst the crack front position appeared uniform across the two faces of the specimen.

The crack resistance curves of the untufted control, copper and stainless steel tufted materials are illustrated in Fig. 4. After crack initiation the curves show a similar, almost linear increase in crack energy release rate for the initial untufted section. The crack initiation toughness is 331 J/m^2 (± 15 J/m^2), 320 J/m^2 (± 15 J/m^2) and 229 J/m^2 (± 31 J/m^2) for the control, copper and stainless steel tufted materials, respectively. There is a slight tendency of reduced initiation toughness of tufted materials which can be attributed to their lower resin volume fraction compared to untufted materials. This results in lower crack initiation toughness as the plastic zone at the crack tip is constrained by adjacent fabric plies. The R-curve of the untufted material reaches a plateau with a crack propagation toughness of 579 J/m^2 (± 110 J/m^2). The crack tip in tufted materials reaches the first tuft row at a crack length of approximately 63 mm (dotted line), is arrested and propagates slowly to the third tuft row in the steel tufted material (dashed line) and fifth or sixth row in the copper tufted material (dashed-dotted line) whilst the delamination toughness increases. Once the first tuft row ruptures the crack propagates until it is arrested again and a fully developed bridging zone is created, indicated by a plateau in the R-curves. The crack propagation toughness, once the bridging zone is

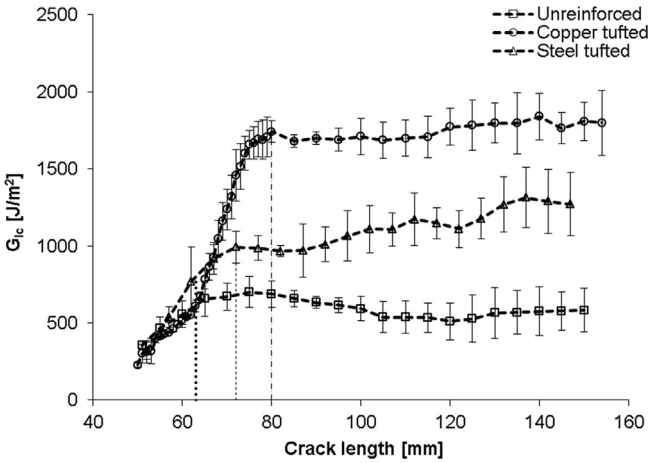

Fig. 4. Delamination fracture toughness vs crack length of bindered composites tufted with copper and stainless steel. Error bars represent one standard deviation.

fully developed, is 1741 J/m^2 (± 138 J/m^2) and 1189 J/m^2 (± 167 J/m^2) for the copper and stainless steel tufted materials, representing an increase of about 200% and 100% compared to the control, respectively. The variations in delamination toughness within the fully developed bridging zone of the tufted materials are caused by the fabric fibre bridging and undulations due to tufting. The crack propagation between stainless steel tufts occurs in an unstable manner, leading to stick-slip behaviour as observed also in [6,13]. However, in the copper tufted material the crack propagates in a stable manner, arrested by up to six tuft rows simultaneously due to the high ductility of the wire, leading to progressive failure. The delamination toughness is governed mainly by the ultimate strain of the thread material which controls the point at which tufts rupture and the accumulated energy is released leading to a higher delamination resistance of about 50% for the copper tufted material compared to the stainless steel tufted composite.

Fig. 5 shows the delamination fracture surface of the control and stainless steel tufted materials. As observed in Fig. 5b tufts rupture at the delamination plane. In addition, some of the non-structural stitches of the fabric fail. During delamination, tufts start debonding from the surrounding composite at the delamination plane. This is followed by axial elongation of the debonded tuft segment and rotational movement of the stainless steel thread due to its twisted architecture. Eventually the tufts rupture. The axial tuft elongation occurring before rupture governs the delamination performance improvements induced by tufting. In addition, tufting influences the delamination behaviour indirectly by enhancing fibre bridging as fibres attached to tufts are elevated during tuft elongation. The effect of fibre bridging is accentuated by the presence of non-structural stitches which can rupture due to bending. In contrast to the delamination fracture surface of tufted specimens, in the untufted material non-structural stitches remain intact and fibre bridging is very limited as shown in Fig. 5a. Fig. 6 highlights the difference in behaviour between copper and stainless steel tufts due to their differences in ductility. The fractured tufts in Fig. 6a are protruding off the delamination plane due to high ductility of the copper wire, whilst the shape of fractured tufts indicates the occurrence of necking. The relatively low ductility of the stainless thread leads to failure without significant elongation as shown in Fig. 6b. This difference in behaviour explains the higher toughness observed in copper tufted materials in comparison to stainless steel tufted composites.

3.2. Lightning strike performance and electrical properties

The measured conductivity of the copper wire and stainless steel thread are 5.4 × 10^7 S/m and 1.2 × 10^6 S/m, respectively. These values are in line with the conductivity of the corresponding bulk material of 5.9 × 10^7 S/m and 1.3 × 10^6 S/m for annealed copper and stainless steel AISI 316L [22,23]. As expected, the through thickness conductivity measurements show a significant increase with metallic tufting. Copper tufting increases the through thickness conductivity of the composite about 250 times, from 21 S/m to 5000 S/m. The increase with the addition of stainless steel tufts is lower with a value of 790 S/m representing an increase of about 20 times in comparison to the control.

Fig. 7 shows the untufted composite panels after Zone 2A lightning strike. The untufted unprotected panel displays the greatest damage in the form of extensive resin burn off and an extended area of fibre fracture and splintering in the centre, as shown in Fig. 7a. The latter type of damage can be considered as critical and could deteriorate the structural integrity of the structure in operation. The small damage regions outside the central area are caused by return strokes of lower current amplitude. Protecting the untufted control panel with a copper mesh reduces the damage significantly, as shown in Fig. 7b. The highly conductive mesh conducts the current along the surface of the composite, reducing the energy density at the attachment location, preventing major fibre fracture and leading to a central area of surface resin burn off and a small amount of out of centre damage caused by return strokes. A small area of fibre fracture present in the centre is caused by the lightning strike in an area that is associated with damage and vaporisation of the copper mesh. This result demonstrates the benefits of the standard solution of incorporating a conductive surface layer in the composite as the type of damage is mostly non critical resin

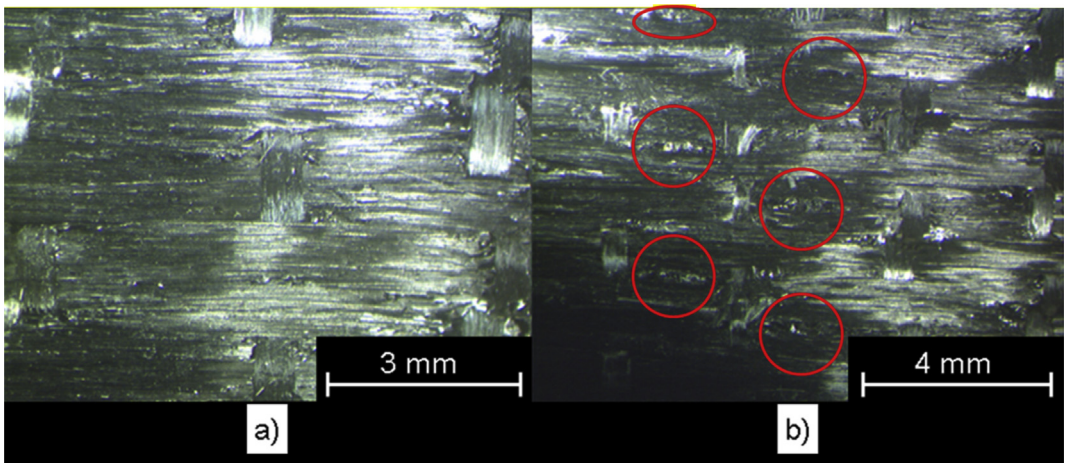

Fig. 5. Optical micrographs of delamination fracture surfaces of (a) untufted control material and; (b) stainless steel tufted material. Steel tufts are circled.

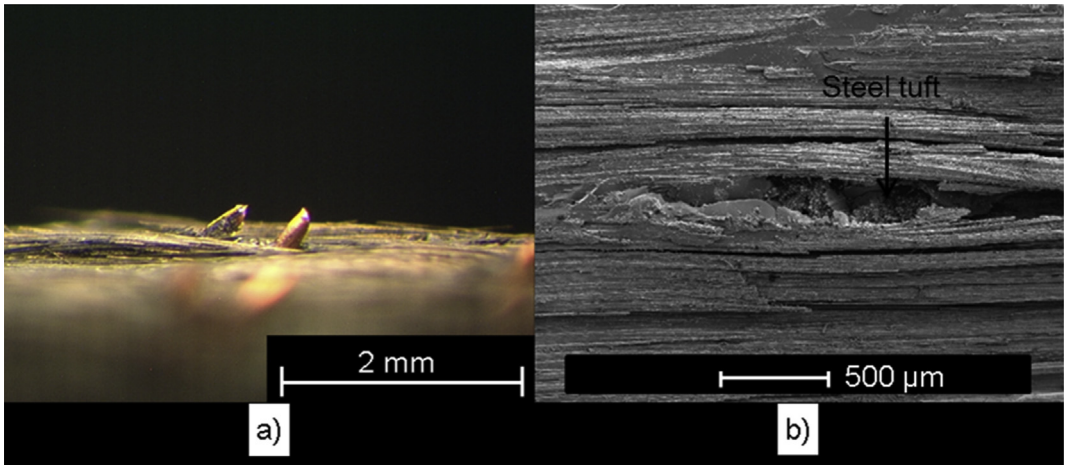

Fig. 6. Fractured tufts at the delamination plane: (a) optical side view of pultruding copper tufts and; (b) scanning electron micrograph of stainless steel tuft failing without significant elongation.

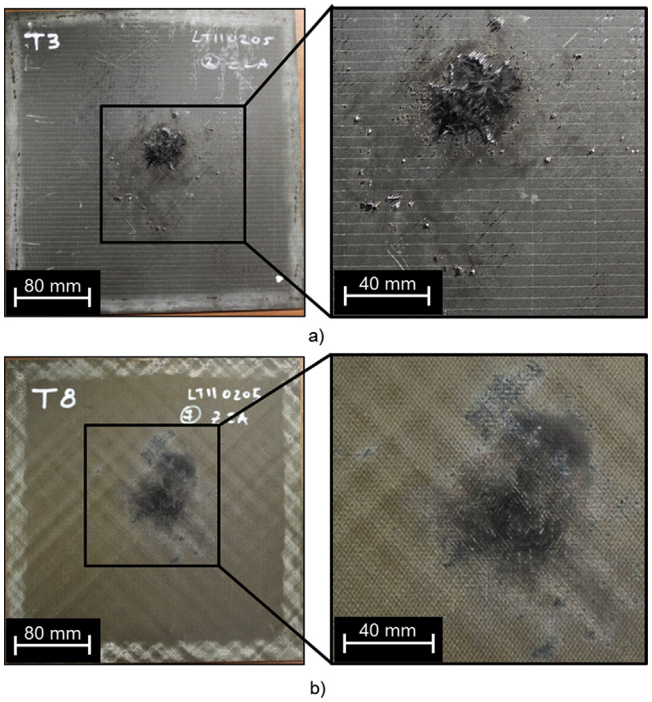

Fig. 7. Composite panels after zone 2A lightning strike: (a) untufted control and (b) untufted control with copper mesh.

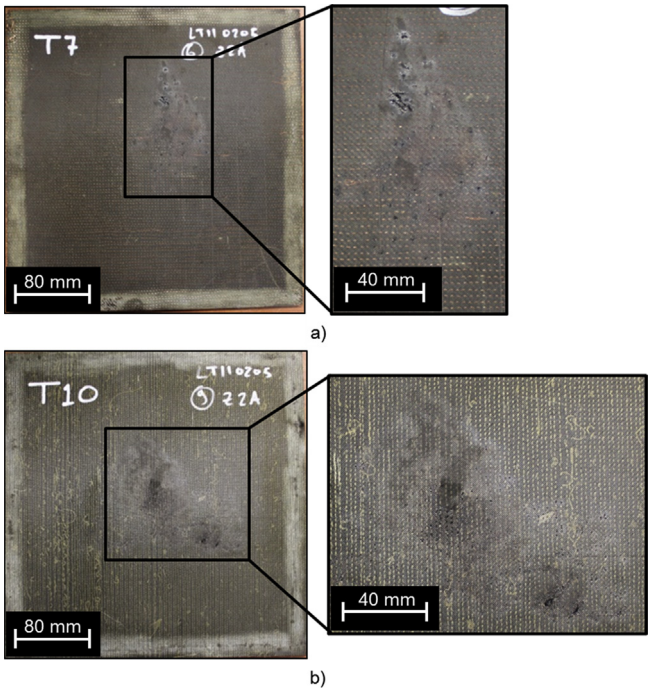

Fig. 8. Composite panels after zone 2A lightning strike: (a) copper tufted and (b) stainless steel tufted.

burn off rather than extensive fibre fracture. The case of the copper tufted composite panel is shown in Fig. 8a. It can be observed that the high conductivity of the copper tufts leads to a very small amount of damage in the centre of the panel accompanied by a few spots of resin burn off away from the centre as a result of return strokes. The current is dissipated successfully through the copper wire tufts leading to significant damage reduction in comparison to the unprotected laminate. Also, the surface damage observed in the copper tufted laminate (Fig. 8a) tends to be lower than that occurring in the copper mesh protected material (Fig. 7b) as a result of current dissipation through the thickness in the case of the tufted material in contrast to through the surface in the case of mesh protection. The results with stainless steel tufts follow a similar trend (Fig. 8b). The panel shows several spots of resin burn off due to return strokes and a small spot of fibre tufting due to the first lightning attachment. The relatively small overall damage, compared to the unprotected control panel is due to the higher through thickness conductivity of the stainless steel laminate. The overall damage in the stainless steel tufted panel appears greater than in the copper tufted material and the mesh protected laminate, which can be attributed to the lower electrical conductivity of steel compared to copper. It should be noted that that the damage areas as identified in Fig. 8 coincide with those identified by C-scan. Therefore, no additional internal damage apart from that identified directly on the surface of the specimens occurred.

The amount of damage, presented in Fig. 9, was quantified by counting the amount of pixels in the corresponding areas. This allowed a distinction between internal and surface damage. Both types of damage correspond to a spectrum of damage types: internal damage can be considered starting from single spots of deep resin burn off up to critical fibre damage, whilst surface damage is manifested by changes in surface colour, such as white and black coloured areas around more crucial damage. The untufted control material without copper mesh (Fig. 7a) shows the largest internal damage area (about 8 cm^2) and

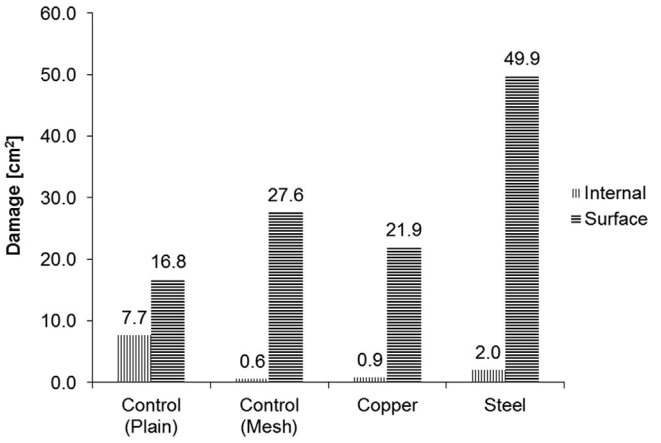

Fig. 9. Size of lightning strike damaged area.

smallest surface damage (17 cm^2). This is due to the limited dissipation of energy on the surface, which leads to transfer of the energy in the through the thickness direction where the low conductivity of the material leads to damage. The internal damage size of the mesh protected material (Fig. 7b) is reduced to approximately 1 cm^2 due to the high conductivity of the mesh and the corresponding dissipation of energy. In this case, the flow of current through the surface causes more extended superficial external damage (about 28 cm^2). The copper tufted panel (Fig. 8a) shows an internal damage size of about 1 cm^2; accompanied by reduced surface damage in comparison to the mesh protected laminate (22 cm^2) due to current dissipation through the thickness leading to the composite with the lowest total damage size. The internal damage area in stainless steel tufted panel (Fig. 8b) is about 2 cm^2, which is significantly reduced compared to the unprotected untufted laminate. However, the relatively low conductivity of the steel leads to increased superficial external damage (about 50 cm^2) compared to copper tufted and mesh protected laminates.

4. Conclusions

Metallic tufts are capable of reinforcing composite structures significantly increasing the delamination toughness in mode I. The tensile behaviour of the tuft has significant impact on the delamination toughness. In the case of the ductile copper wire the high ultimate strain allows several tuft rows to bridge the crack simultaneously leading to very high delamination toughness and progressive failure. The incorporation of metallic tufts increases significantly the through the thickness conductivity of composites. This is reflected in significantly better lightning strike performance, which in the case of copper tufting matches the performance of standard protection methods such as the use of copper mesh. Furthermore, the use of tufting changes significantly the electrical behaviour during lightning strike as current can be dissipated through the thickness in contrast to surface dissipation which is dominant in standard protection methods. This leads to a reduction in surface damage.

This work shows that use of metallic tufting and especially ductile high electrical conductivity materials improves significantly both the mechanical and the lightning strike behaviour of carbon fibre composites. Therefore, metal tufted carbon composites present a unique solution in high end applications requiring both advanced mechanical and electrical performance. The manufacturing flexibility associated with tufting generates further opportunities for utilisation of such a solution in a selective and optimised manner within a structure with emphasis on joints, dissimilar joints, areas subjected to loading conditions leading to through thickness failure and potential lightning strike attachment locations.

Acknowledgments

This work was supported by the Engineering and Physical Sciences Research Council, through the EPSRC Centre for Innovative Manufacturing in Composites (CIMComp: EP/IO33513/1).

Appendix A. Supplementary data

Data underlying this study can be accessed through the Cranfield University repository at https://dx.doi.org/10.17862/cranfield.rd.5484079.

References

[1] Cartié DDR, Dell'Anno G, Poulin E, Partridge IK. 3D reinforcement of stiffener-to-skin T-joints by Z-pinning and tufting. Eng Fract Mech 2006;73:2532–40.
[2] Mouritz AP. Delamination properties of z-pinned composites in hot-wet environment. Compos Part A Appl Sci Manuf 2013;52:134–42.
[3] Pingkarawat K, Mouritz AP. Stitched mendable composites: balancing healing performance against mechanical performance. Compos Struct 2015;123:54–64.
[4] Dransfield KA, Jain LK, Mai Y-W. On the effects of stitching in CFRPs—I. Mode I delamination toughness. Compos Sci Technol 1998;58:815–27.
[5] Koissin V, Kustermans J, Lomov SV, Verpoest I, Van Den Broucke B, Witzel V. Structurally stitched NCF preforms: quasi-static response. Compos Sci Technol 2009;69:2701–10.
[6] Colin de Verdiere M, Skordos AA, May M, Walton AC. Influence of loading rate on the delamination response of untufted and tufted carbon epoxy non crimp fabric composites: mode I. Eng Fract Mech 2012;96:11–25.
[7] Dell'Anno G, Cartié DD, Partridge IK, Rezai A. Exploring mechanical property balance in tufted carbon fabric/epoxy composites. Compos Part A Appl Sci Manuf 2007;38:2366–73.
[8] Colin de Verdiere M, Pickett AK, Skordos AA, Witzel V. Evaluation of the mechanical and damage behaviour of tufted non crimped fabric composites using full field measurements. Compos Sci Technol 2009;69:131–8.
[9] Dell'Anno G. Effect of tufting on the mechanical behaviour of carbon fabric/epoxy composites. Cranfield University; 2007.
[10] Dell'Anno G, Partridge I, Cartié D, Hamlyn A, Chehura E, James S, et al. Automated manufacture of 3D reinforced aerospace composite structures. Int J Struct Integrity 2012;3:22–40.
[11] Treiber WG, Cartié DDR, Partridge IK. Determination of crack bridging laws in tufted composites. In ICCM-17 Int. Conf. Compos. Mater. Edinburgh, UK; 2009.
[12] Mills AR, Jones J. Investigation, manufacture, and testing of damage-resistant airframe structures using low-cost carbon fibre composite materials and manufacturing technology. Proc Inst Mech Eng Part G J Aerosp Eng 2010;224:489–97.
[13] Treiber JWG. Performance of tufted carbon fibre/epoxy composites. Cranfield University; 2011.
[14] Henao A, Carrera M, Miravete A, Castejón L. Mechanical performance of through-thickness tufted sandwich structures. Compos Struct 2010;92:2052–9.
[15] Davis M, Bond D. Principles and practices of adhesive bonded structural joints and repairs. Int J Adhes Adhes 1999;19:91–105.
[16] Kumar SB, Sivashanker S, Bag A, Sridhar I. Failure of aerospace composite scarf-joints subjected to uniaxial compression. Mater Sci Eng A 2005;412:117–22.
[17] Kweon JH, Jung JW, Kim TH, Choi JH, Kim DH. Failure of carbon composite-to-aluminum joints with combined mechanical fastening and adhesive bonding. Compos Struct 2006;75:192–8.
[18] Welch JM. Repair design, test, and process considerations for lightning strikes. In CACRC/MIL-HDBK-17 Conf. Amsterdam, Netherlands; 2007.
[19] Kawakami H, Feraboli P. Lightning strike damage resistance and tolerance of scarf-repaired mesh-protected carbon fiber composites. Compos Part A Appl Sci Manuf 2011;42:1247–62.
[20] Haynes K.K. CM. Lightning strike protection: novel nonwoven technology. JEC Compos 2006;24:32–3.
[21] Klomp-de Boer R, Smeets M. Lightning strike behaviour of thick walled resin transfer moulded parts using various lightning strike protection concepts. Amsterdam, Netherlands; 2013.
[22] Matula RA. Electrical resistivity of copper, gold, palladium, and silver. J Phys Chem Ref Data 1979;8:1147–298.
[23] Ho CY, Chu TK. Electrical resistivity and thermal conductivity of nine selected AISI stainless steels. DTIC Document. 1977.